ACS OMEGA

http://pubs.acs.org/journal/acsodf

Article

Design of a Structurally Novel Multipotent Drug Candidate by the Scaffold Architecture Technique for ACE-II, NSP15, and M^{pro} Protein Inhibition: Identification and Isolation of a Natural Product to Prevent the Severity of Future Variants of Covid 19 and a Colorectal Anticancer Drug

Sourav Pakrashy, Prakash K. Mandal, Surya Kanta Dey, Sujata Maiti Choudhury, Fatmah Ali Alasmary, Amani Salem Almalki, Md Ataul Islam, and Malay Dolai*

Cite This: *ACS Omega* 2022, 7, 33408−33422

Read Online

ACCESS | Metrics & More | Article Recommendations | Supporting Information

ABSTRACT: Scaffold architecture in the sectors of biotechnology and drug discovery research include scaffold hopping and molecular modelling techniques and helps in searching for potential drug candidates containing different core structures using computer-based software, which greatly aids medicinal and pharmaceutical chemistry. Going ahead, the computational method of scaffold architecture is thought to produce new scaffolds, and the method is capable of helping search engines toward producing new scaffolds that are likely to represent potent compounds with high therapeutic applications, which is a possibility in this case as well. Here we probate a different interactive design by natural product hopping, molecular modelling, pharmacophore modelling, modification, and combination of the phytoconstituents present in different medicinal plants for developing a pharmacophore-guided good drug candidate for the variants of SARS-CoV-2 or Covid 19. In the modern era, these approaches are carried out at every level of development of scaffold queries, which are increasingly summarized from chemical structures. In this context, we report on a successfully designed drug-like candidate having a high-binding-affinity "compound SLP" by understanding the relationships between the compounds' pharmacophores, scaffold functional groups, and biological activities beyond their individual applications that abide by Lipinski's rule of five, Ghose rule, Veber rule etc. The new scaffold generated by altering the core of the known phyto-compounds holds a good predicted ADMET profile and is examined with iMODS server to check the molecular dynamics simulation with normal mode analysis (NMA). The scaffold's three-dimensional (3D) structure yields a searchable natural product koenimbine from a conformer database having good ADMET property and high availability in spice *Murraya koenigii* leaves. *M. koenigii* leaves are easily available in the market, and might ensure the immunity, good health, and well-being of people if affected with any of the variants of Covid 19. The cell viability studies of koenimbine on murine colorectal carcinoma cell line (CT-26) showed no toxicity on normal mice lymphocyte cells (MLCs). The anticancer mechanism of koenimbine was displayed by its enhanced capacity to produce intercellular reactive oxygen species (ROS) in the colorectal carcinoma cell line.

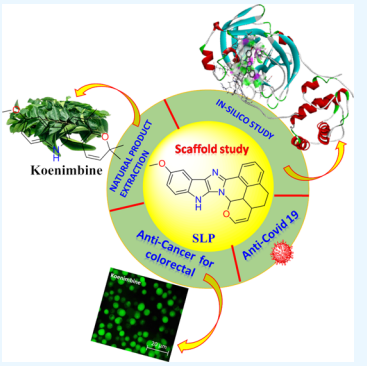

INTRODUCTION

Before the discovery of modern medicines in the field of allopathy, in the ancient era, treating patients was an individual practice and doctors used to treat sick people with medicines obtained from nature, most of which were from medicinal plants or may be referred to as herbal drugs. Moreover, at that time, a huge amount of vegetation was sufficient to cater to their needs. It was believed that the efficiency of the plant medicines depends on the wholesome composition of the plant or a certain plant part. In the modern era, where isolation of phytoconstituents using chromatographic techniques and their structural elucidation are possible using nuclear magnetic resonance (NMR) and X-ray diffraction (XRD), one can easily find out the structure of molecules present in a medicinal plant; also, with the development of biotechnology and biochemistry, the activity of a concerned structure can be easily studied. We aim to prepare a successful drug candidate that has the ability to bind at the active sites of the proteins and enzymes that help in the survival and replication of the Covid 19 virus by modifying the active ingredient using the

Received: July 2, 2022
Accepted: August 30, 2022
Published: September 10, 2022

scaffold architecture technique of the medicinal plant to make it better and easy to synthesize a drug molecule.

The active structures from medicinal plants have always paved the way to the development of drugs, and the objective of our study is to prepare a new drug candidate from raw plant secondary metabolites or active ingredients. We also consider other issues like the presence of heavy metals, α toxin residues, and specific pathogens while performing a molecular similarity search for an easily available food or spice having a similar natural product. As mentioned, computational advancements in biotechnology like the scaffold hopping method are applied to the new drug candidate and the method is capable of helping search engines toward producing new scaffolds that are likely to represent potent compounds with high therapeutic applications, which is a possibility in this case as well.

The Covid 19 virus has a spike glycoprotein that encourages the entry of human angiotensin-converting enzyme 2 (ACE2) receptor;[1] thus, if we can make a drug molecule that can bind to Spike-receptor-binding domain-ACE2 (Spike-RBD-ACE2) in a better way than the virus, then it can be seen as a good strategy to control the spread of infection. Along with these persuasions, a cysteine protease (3-chymotrypsin-like protease (3CLpro) or the main protease (M^{pro})) is found necessary for the viral life cycle of the Covid 19 virus.[2] Of functional importance is another protein as well that is responsible for the survival and replication of the virus; it is an enigmatic protein, an endo-ribonuclease that is highly needed for protein interference, called NSP15.[3] Therefore, these three proteins were taken as fugitive targets for developing a potential drug candidate.

MATERIALS AND METHODS

Data Collection. Here the study was conducted by choosing compounds that are active ingredients of several medicinal plants, the native N3 ligand of 6LU7 protein, molnupiravir, and ivermectin[4] as controls and chloroquine. The molecules belonging to the respective medicinal plant are individually considered for molecular docking study with all of the protein targets.

Molecular Docking. The in silico docking of the compounds, which is called the protein−ligand binding energy (ΔG) analysis, was performed using AutoDock Vina[5] as an extension in UCSF Chimera.

The protein human ACE2-receptor, Nsp15 endo-ribonuclease, and M^{pro} were retrieved from RCSB Protein DataBank (PDB) (http://www.rcsb.org/pdb), PDB-ID 1R4L, 6VWW, and 6LU7 in PDB format. As per the docking protocol, removal of all water and solvent molecules, co-crystallized residues, and mirror chain (if any) was ensured using UCSF Chimera software. The next part is the protein structure preparation, which is also done in Chimera. The protein structures were prepared by assigning the hydrogen atoms, charges, and energy minimization using DockPrep tool. The charges were assigned as per the AM1-BCC method, which quickly and efficiently generates high-quality atomic charges for the protein, and the charges were computed using ANTECHAMBER algorithm.[6] The energy minimization was performed using 500 steepest descent steps with 0.02 Å step size with an update interval of 10. The protein energy minimization of 6LU7 was further done with SwissPDB viewer[7] as it contained a co-crystallized ligand. The target proteins after minimization of energy were then saved in PDB format for docking purpose.

All of the ligands used for the in silico interaction assays were mostly the medicinal plants' secondary metabolites and the structures that were present in PubChem were retrieved from there in SDF format along with the control of 6LU7, which is the N3 ligand, and 1R4L, which is Ivermectin, while others were directly drawn on ChemDraw; these drawn structures were copied to Chem3D pro, where their energy minimization was carried out using MM2 calculations (not for float structures). After that, they were saved in SDF format. Before performing the molecular docking of the ligand and protein, the ligands were optimized by addition of hydrogen and addition of charges using the Gasteiger algorithm.[8] Energy minimization was performed using 1000 steepest descent steps with 0.02 Å step size with an update interval of 10 and then again saved in PDB format using the structure editing wizard of Chimera software, which is driven by the chemoinformatic principle of electronegativity equilibration; then the files were saved in PDB format. A grid box that assigns the binding region was chosen in such a way that it would cover the protein's active site for the hydrophobic surface of the concave region of the protein to fit in properly the hydrophobic surface of the ligand, giving the best binding score.

New molecules were designed by altering the architecture of the best-fit active phytoconstituents in two-dimensional (2D) format first using ChemDraw ultra-software, and then copying and pasting them in Chem3D pro to convert them to 3D SDF format after minimizing the energy of the molecules using MM2. The rest of the method of preparation of the molecules as ligands for docking is the same as above. For visualizing in different formats, we used the software Discovery studio and UCSF Chimera.

Scaffold Architecture. Scaffold architecture heir's new scaffolds utilize many aspects to replace active natural compounds with synthetic equivalents that are chemically easier to access. To this end, it is an attractive similarity-based computational approach typically attempted by pharmacophore-guided interactive designs capable of detecting compounds with different core structures having the same or enhanced activity and reliable absorption, distribution, metabolism, and excretion (ADME) properties. This method gently modulates the core structure of a natural product with different functional moieties such that the local or global similarity remains intact to a greater percentage while chemical and biological activities get enhanced.

Molecular Similarity Finding. Molecular similarity findings mainly depend on the similarity property principle, which means similar properties are shown by compounds that are similar chemically and structurally. In this study, the property chosen is predictive biological activity on the basis of the docking score with targeted proteins. Physicochemical descriptors like log P, molecular weight, number of rotatable bonds etc., which are generally defined as mathematical models of chemical properties, are also taken into account. Similarity computed with compound SLP using ZINC software yields a significantly large number of compounds, most of which are either synthetic or semisynthetic.

Along with computational help, we also considered human perception and searched the secondary metabolites of medicinally important spices and foods.

All of the selected candidates were then subjected to docking analysis. The molecule that passed at least two control parameters and showed good ADME properties as predicted

https://doi.org/10.1021/acsomega.2c04051
ACS Omega 2022, 7, 33408−33422

Scheme 1. Schematic Presentation of the Probable Synthetic Pathway of the Molecule "SLP"

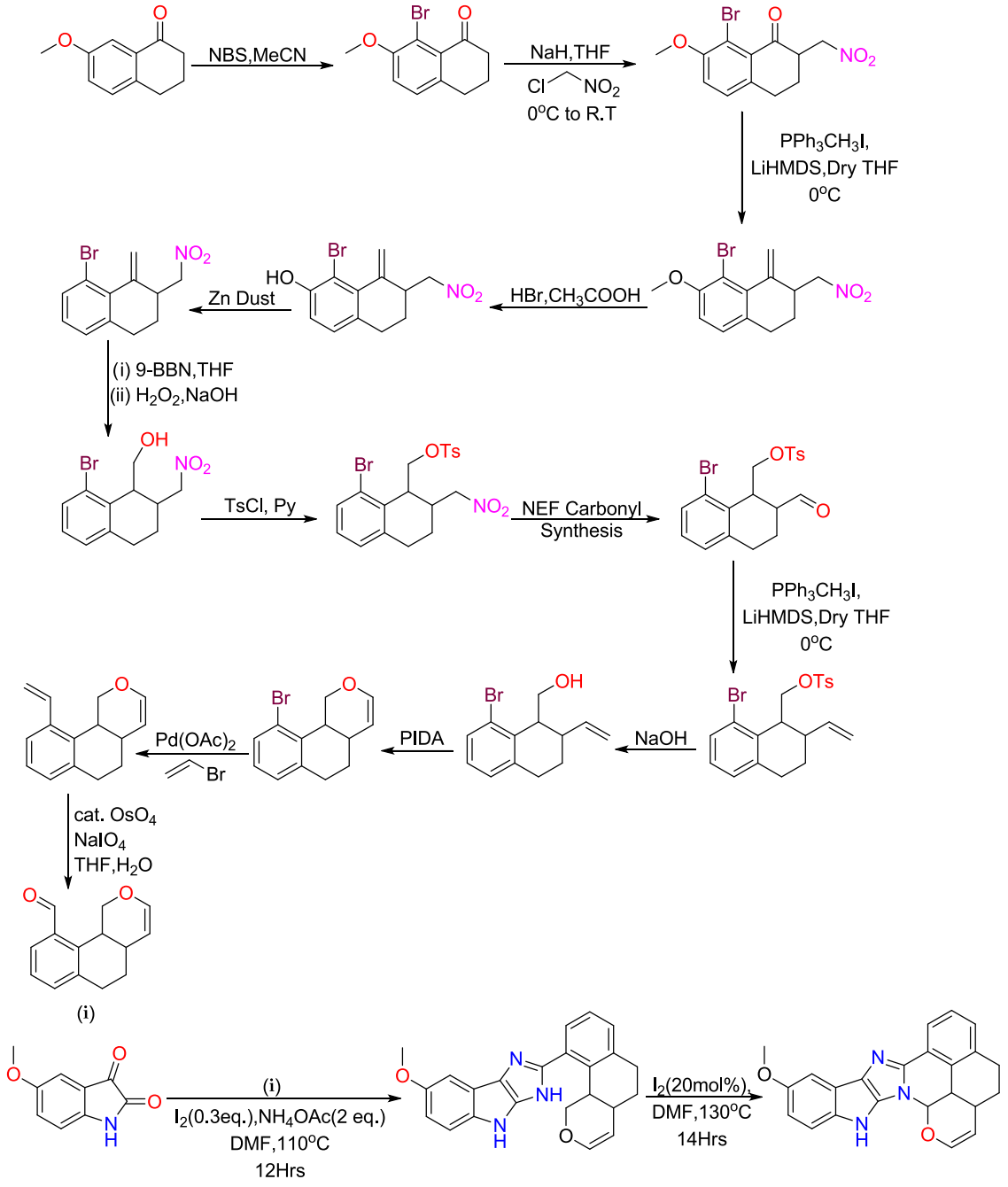

by SwissADME software was then chosen as the alternative of compound SLP.

ADMET Prediction. In silico ADME analysis was conducted to investigate the physicochemical properties of the potent hits, such as water solubility, lipophilicity, and pharmacokinetics, by using the website http://www.swissadme.ch,[9] but the toxicity of these molecules cannot investigated by using SwissADME, so the help of pk-CSM[10]—a pharmacokinetics server—was taken to predict the toxicity properties of the molecules with their SMILE (Simplified Molecule Input Line Entry Specification) profile.

Isolation of the Natural Product (Koenimbine). The leaves of *M. koenigii* Spreng. (Rutaceae) (100 g), commonly known as "Kurry patta" or "curry patta" in India, which is the only part that people consume, grow throughout India and also in the Andaman Islands, collected from the local markets of West Bengal, India, were air dried and extracted with 1% ethylacetate in *n*-hexane in a Soxhlet apparatus for 72 h. The total extract was concentrated using a rotary evaporator and kept at room temperature for some time, then weighed, and found to have 1.22 g of a yellowish solid. This was dissolved in chloroform and chromatographed using a silica gel column and eluted with 2% ethylacetate in *n*-hexane.

The fraction obtained with 2% ethylacetate in *n*-hexane afforded a white solid, which after washing with *n*-hexane afforded 290 mg of pure koenimbine as a white buff solid; the structure was confirmed using ^{1}H-NMR. So the amount of koenimbine present in the leaves of *Murraya koenigii* is found to be 0.029%. The melting point was determined in open

https://doi.org/10.1021/acsomega.2c04051
ACS Omega 2022, 7, 33408−33422

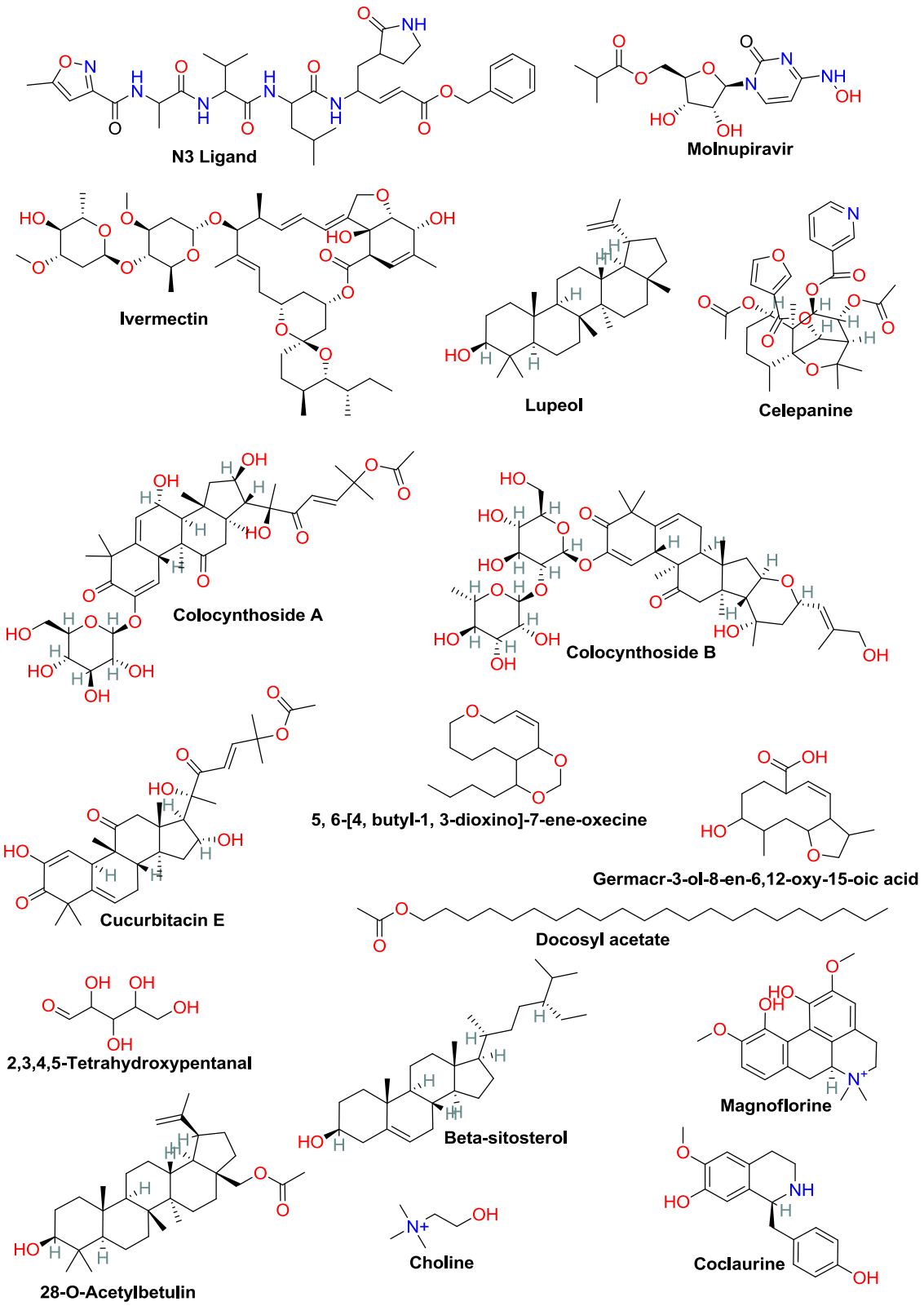

Figure 1. Structures of active ingredients of several medicinal plants from Table 1.

capillary tubes in a Köfler block apparatus and found to be 194.6 °C.

^{1}H-NMR δ($CDCl_3$): 1.49 (6H, s, H-2′a/H-2′b), 2.33(3H, s, H-3a), 3.91 (3H, s, H-6a), 5.71 (1H, d, J = 10.0 Hz, H-3′), 6.63 (1H, d, J = 10.0 Hz, H-4′), 6.97(1H, dd, J = 10.0, 3.0 Hz, H-7), 7.29 (1H, d, J = 10.0 Hz, H-8), 7.42 (1H, d, J = 3.0 Hz, H-5), 7.63 (1H, s, H-4), 7.71 (1H, br.s, >NH). (Figure S1 in SI)

Probable Synthetic Pathway of Our Designed Molecule SLP. The designed molecule SLP can be synthesized from the easily available 7-methoxy-α-tetralone; bromination of the commercially available molecule is carried

https://doi.org/10.1021/acsomega.2c04051
ACS Omega 2022, 7, 33408−33422

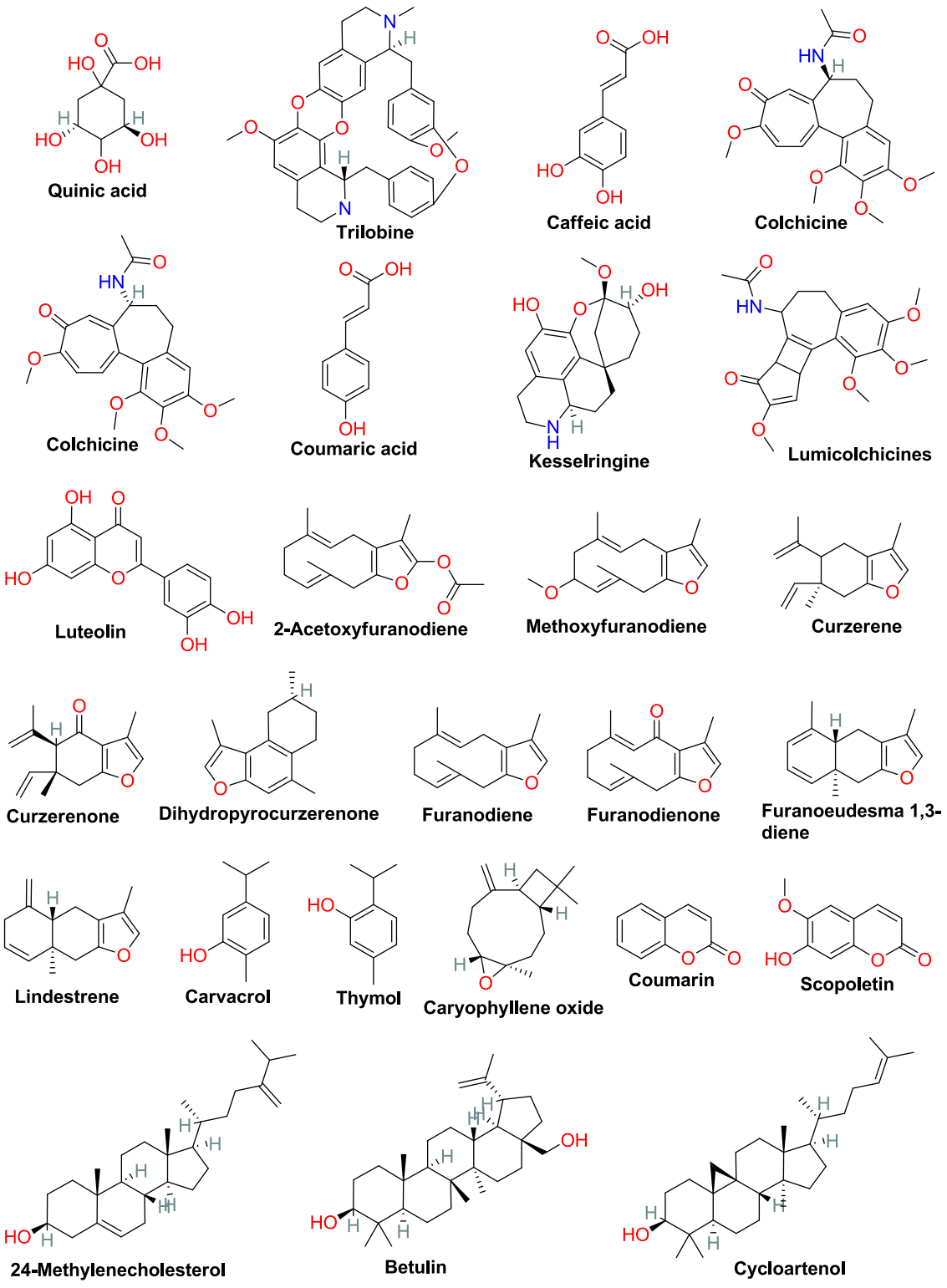

Figure 2. Structures of the active ingredients of several medicinal plants from Table 1.

out with NBS (*N*-bromosuccinaamide) in acetone, followed by a series of steps (Scheme 1) to produce (i), which on treatment with 5-methoxy acetone in the presence of iodine and ammonium acetate with DMF solvent and heating to 110 °C for 12 h[11] produces our precursor molecule. Lastly, in the same reaction tube we added 20 mol % iodine and heated it at 130 °C for 14 h more.

Molecular Dynamics Simulation. Molecular dynamics simulation study of docked complexes plays a crucial part to validate the drug candidate and protein fit binding, molecular dynamics were carried out with iMODS server to explain the usual protein motion within the internal coordinates through normal mode analysis (NMA). iMODS[12] is a highly customizable and useful server and shows a number of levels which are coarse grained (CG). It predicts the dihedral coordinates of

https://doi.org/10.1021/acsomega.2c04051
ACS Omega 2022, 7, 33408−33422

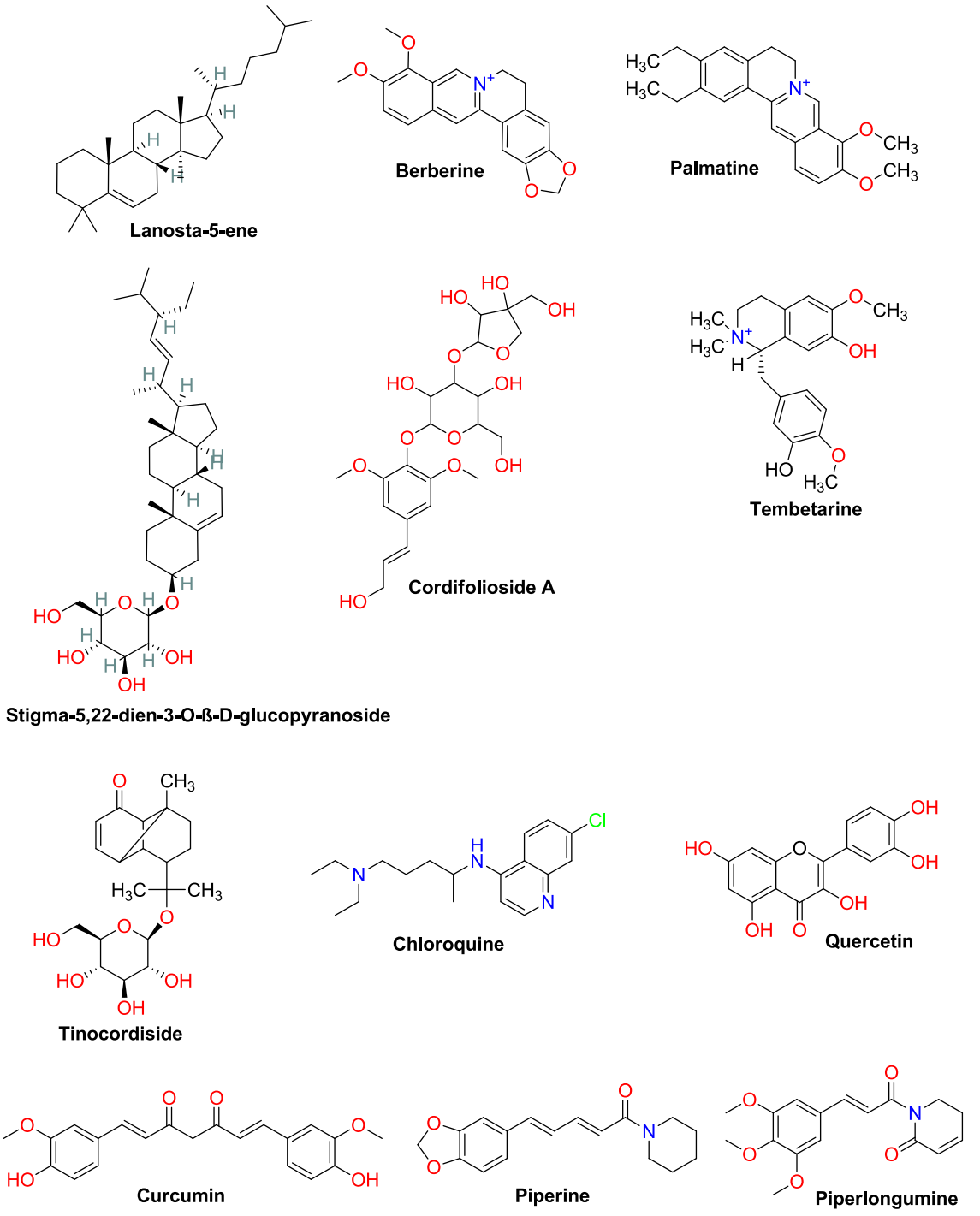

Figure 3. Structures of active ingredients of several medicinal plants and chloroquine from Table 1.

Cα atoms with large calculations of these big docked complexes. Furthermore, the B-factor is also predicted in the iMODS server along with structural deformability and determines eigenvalue.

Cell Viability Study of Koenimbine on Mice Lymphocyte Cells (MLCs) and the Murine Colorectal Carcinoma Cell Line (CT-26). The detailed methods and experiments of the cell viability study of koenimbine on MLCs and on CT-26 are given in the SI file.

Measurement of Intracellular ROS Generation. Intracellular ROS generation was measured using 2′,7′-dichlorodihydrofluorescein diacetate (H_2DCFDA).[13] CT-26 cells were treated with Koenimbine at its IC_{50} dose (20.47 μg/mL) for 24 h. After that, Dulbecco's modified Eagle medium (DMEM) was discarded; the cells were washed with phosphate-buffered saline (PBS, pH 7.4) and incubated with H_2DCFDA (1 μg/mL) for 30 min at 37 °C, then washed with PBS three times. Finally, oxidation of DCFH-DA to 2′-7′dichlorofluorescein (DCF) was quantified using a Hitachi F-7000 fluorescence spectrophotometer at 485 nm (excitation) and 520 nm (emission). The image was recorded by fluorescence microscopy (LEICA DFC295, Germany). 5-Fluorouracil (5-FU) was used as positive control.

https://doi.org/10.1021/acsomega.2c04051
ACS Omega 2022, 7, 33408−33422

Table 1. Results of the Docking of Control Molecules, Secondary Metabolites, and Chloroquine

name and structure	pubchem ID	docking score 6LU7	6VWW	1R4L
control 1: N3 ligand	146025593	−6.9		
control 2: molnupiravir	145996610	−6.8	−7.0	
control 3: ivermectin	6321424			−10.9
(1) lupeol	259846	−7.3	−7.5	−9.8
(2) celepanine	442518	−7.1	−7.4	−8.7
(3) 5,6-[4-butyl-1,3-dioxino]-7-ene-oxecine		−5.9	−5.5	−6.9
(4) choline	305	−3.7	−3.8	−3.5
(5) colocynthoside A	16216752	−8.1	−8.3	−10.3
(6) colocynthoside B	16216649	−7.3	−8.1	−10.2
(7) cucurbitacin E	5281319	−7.4	−8.4	−10
(8) docosyl acetate	69969	−4.4	−3.9	−5.6
(9) germacr-3-ol-8-en-6,12-oxy-15-oic acid		−6.6	−6.3	−8
(10) 2,3,4,5-tetrahydroxypentanal	854	−4.5	−5.2	−5.6
(11) 28-*O*-acetylbetulin	14038495	−7.8	−8.2	−9
(12) *β*-sitosterol	222284	−7.5	−8.1	−9.4
(13) coclaurine	160487	−7.5	−7.7	−8.5
(14) magnoflorine	73337	−6.9	−7.7	−10
(15) quinic acid	6508	−5.4	−6.4	−6.6
(16) trilobine	169007	−8.4	−9.3	−10.5
(17) caffeic acid	689043	−6	−6.7	−6.5
(18) colchicine	6167	−6.2	−6.9	−7.8
(19) colchimine		−6.6	−7.5	−8.4
(20) coumaric acid	637542	−6	−6.2	−6.1
(21) kesselringine	76967674	−7.3	−7.9	−8.6
(22) lumicolchicines	244898	−6.9	−6.7	−7.5
(23) luteolin	5280445	−7.4	−8.3	−8.6
(24) 2-acetoxyfuranodiene	91748044	−7	−7.3	−8.4
(25) 2-methoxyfuranodiene	6325622	−6.3	−6.3	−7.9
(26) curzerene	572766	−5.7	−6.1	−7.1
(27) curzerenone	3081930	−6.1	−7	−7.3
(28) dihydropyrocurzerenone	91734838	−6.3	−7	−8.1
(29) furanodiene	9601230	−5.9	−7.1	−7.4
(30) furanodienone	6442374	−6.3	−6.4	−7.7
(31) furanoeudesma 1,3-diene	643237	−6.6	−7.1	−8.2
(32) lindestrene	12311270	−6.4	−7.7	−8.3
(33) 24-methylenecholesterol	92113	−7.9	−8.1	−9.6
(34) betulin	72326	−7.3	−7.5	−9.5
(35) carvacrol	10364	−5.2	−6	−6
(36) caryophyllene oxide	1742210	−6.3	−6.1	−7.1
(37) coumarin	323	−5.6	−6.4	−6.4
(38) cycloartenol	92110	−7.4	−8.3	−10.4
(39) lanosta-5-ene	123204535	−6.9	−7.8	−9.9
(40) scopoletin	5280460	−5.7	−6.4	−7
(41) stigma-5,22dien-3-*O*-ß-D-glucopyranoside	6602508	−6.9	−9	−9.8
(42) thymol	6989	−4.9	−6.6	−6.2
(43) berberine	2353	−7.5	−7.7	−8.2
(44) cordifolioside A	75111036	−7.1	−7.1	−8.4
(45) palmatine	19009	−7	−7	−8
(46) tembetarine	167718	−6.4	−7.1	−8.6
(47) tinocordiside	177384	−7.6	−8.2	−9.7
(48) chloroquine	2719	−5.7	−6.1	−7
(49) quercetin	5280343	−7.2	−8	−8.4
(50) curcumin	969516	−6.7	−8.4	−9.3
(51) piperine	638024	−6.6	−7.8	−8.3
(52) piperlongumine	637858	−6.1	−7.1	−8.1

RESULTS

Docking Results. *Docking Studies.* The protein−ligand binding interactions between the targeted proteins PDB-ID 6LU7, 6VWW, and 1RL4 and the ligands, which are mainly phytoconstituents of medicinal plants, were found out using molecular docking. The calculations reveal the highest free energy change for these interactions as $\Delta G = -8.4$ kcal/mol for trilobine for Protein M^{pro} 6LU7 inside a grid box of −10.75 Å × 12.33 Å × 68.84 Å with size 30 Å × 30 Å × 30 Å along the *x*-, *y*-, and *z*- axes. For Protein Nsp15 endo-ribonuclease 6VWW, predicted calculations reveal the free energy change for these interactions as $\Delta G = -9.3$ kcal/mol for trilobine inside a grid box of −67 Å × 30 Å × 26 Å with size 30 Å × 30 Å × 30 Å along the *x*-, *y*-, and *z*- axes. For Protein Human ACE2-receptor (A-Chain) 1R4L, predicted calculations reveal the free energy change for these interactions as $\Delta G = -10.5$ kcal/mol for trilobine inside a grid box of 38 Å × 2 Å × 26 Å with size 71 Å × 56 Å × 59 Å along the *x*-, *y*-, and *z*-axes (Figures 1−3 and Table 1).

Scaffold Architecture. Trilobine showed the best binding among all other phytoconstituents chosen in this case. It binds better than the control molnupiravir and N3 ligand. but less effective than the control Ivermectin, so we architected a new design by altering the structure of trilobine so that we can make a new and improved drug candidate for Covid 19 (Figure 4).

The newly designed molecule SLP showed better protein−ligand binding interactions with the targeted proteins 6LU7 (inside a grid box of −10.75 Å × 12.33 Å × 68.84 Å with size 30 Å × 30 Å × 30 Å along the *x*-, *y*-, and *z*-axes), 6VWW (inside a grid box of −67 Å × 30 Å × 26 Å with size 30 Å × 30 Å × 30 Å along the *x*-, *y*-, and *z*-axes), and 1RL4 (inside a grid box of 38 Å × 2 Å × 26 Å with size 71 Å × 56 Å × 59 Å along the *x*-, *y*-, and *z*- axes) than the control molecules, as evidenced from its docking scores given in Table 2, and it can easily be synthesized in a lab or industry at a low cost (Figures 5−7).

Molecular Similarity Finding. However, time is an important factor, and as we know, the time requirement is quite high to bring a new drug molecule into the market since it has to pass lots of parameter tests, which are highly necessary. In order to meet the rush, we discovered a molecule that showed high molecular, structural, chemical, biological, and local similarities like the number of rotatable bonds, H-bond acceptors, and H-bond donors etc. to the known spice *M. koenigii* Spreng. (Rutaceae) and can be consumed every day since it has much availability; it also showed better binding than controls 1 and 2 (evidenced in Table 3) and thus can be used to combat the virus causing Covid 19 (Figure 8).

Koenimbine is a natural product and has good molecular similarity to our designed compound SLP. It is available in the spice *M. koenigii*, which along with koenimbine has a lot of other active components as well; so it can be a good choice of food on the table during Covid 19 disease (Figures 9−11).

Cell Viability Study of Koenimbine on Mice Lymphocyte Cells (MLCs) and the Murine Colorectal Carcinoma Cell Line (CT-26). The cell viabilities of MLCs and CT-26

https://doi.org/10.1021/acsomega.2c04051
ACS Omega 2022, 7, 33408−33422

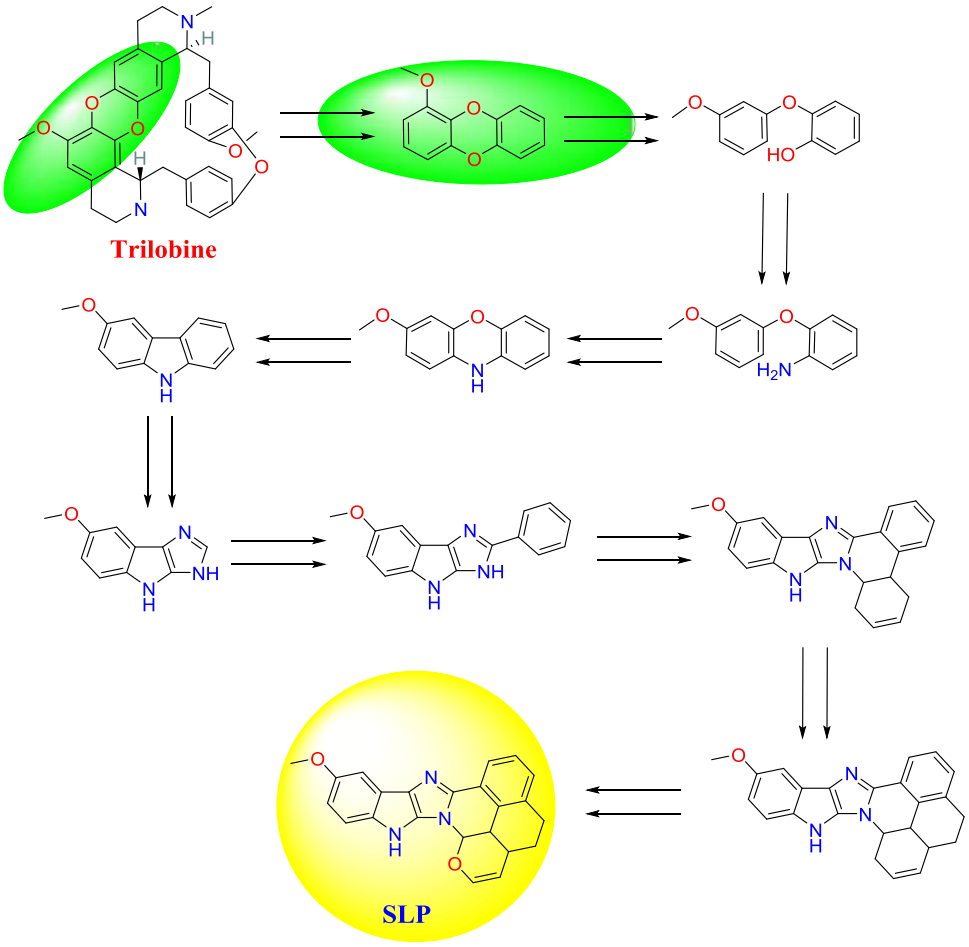

Figure 4. Scaffold architecture of SLP from trilobine.

Table 2. Docking Score of the SLP Molecule

name and structure	pubchem ID	docking score		
		6LU7	6VWW	1R4L
SLP		−8.5	−9.9	−11.4

cells were studied by MTT assay. The results showed that koenimbine significantly inhibited CT-26 cells' viability in a concentration-dependent manner as compared to the CT-26 control group (Figure 12). As the concentration was increased, the growth of cells seemed to be decreased and the IC_{50} value

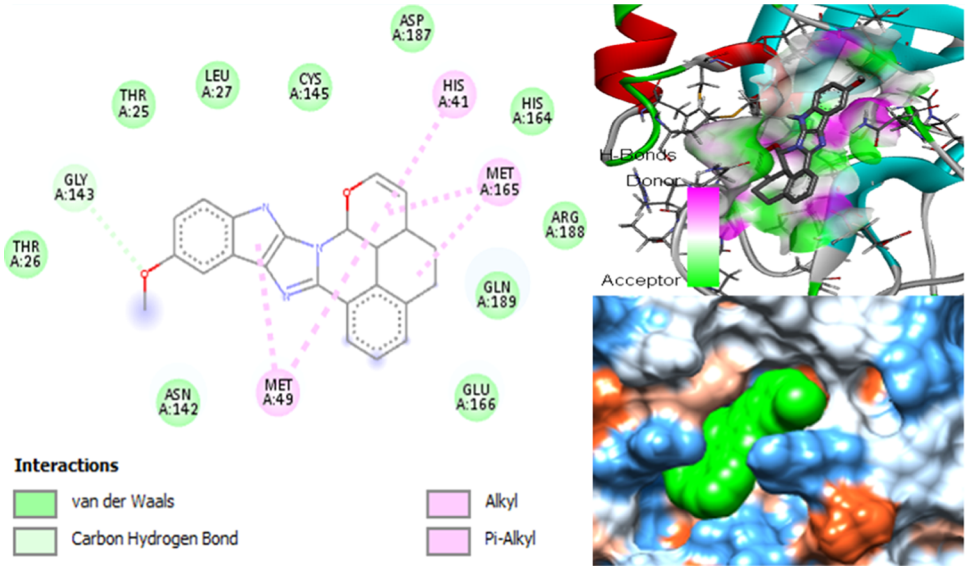

Figure 5. Docking poses of SLP with 6LU7.

https://doi.org/10.1021/acsomega.2c04051
ACS Omega 2022, 7, 33408−33422

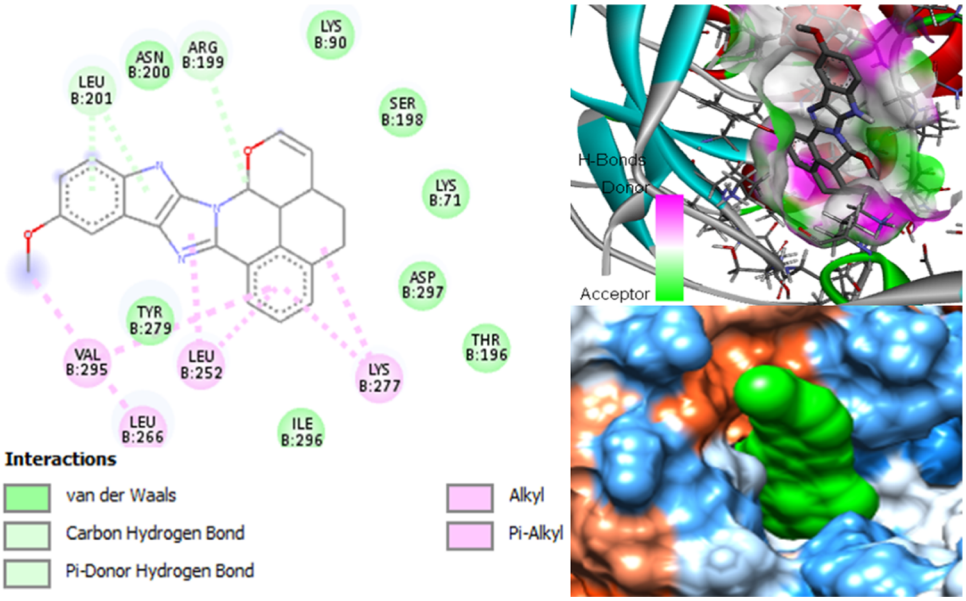

Figure 6. Docking poses of SLP with 6VWW.

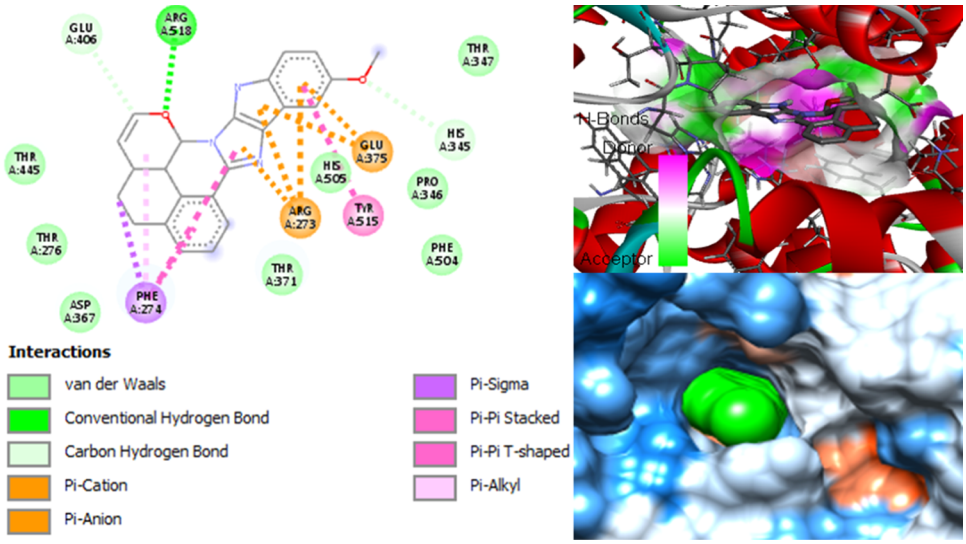

Figure 7. Docking poses of SLP with 1R4l.

Table 3. Results of the Docking of Koenimbine

		docking score		
name and structure	pubchem ID	6LU7	6VWW	1R4L
koenimbine	97487	−7.1	−7.9	−9.3

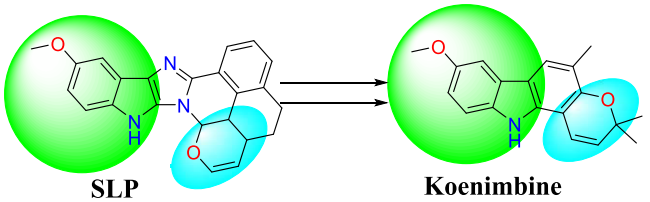

Figure 8. Molecular, structural, chemical, biological, and local similarities of koenimbine with SLP.

of koenimbine was found to be 20.47 ± 2.48 μg/mL. However, the IC_{50} value of 5-FU was 14.57 ± 3.08 μg/mL, which is significantly ($^{\#\#}p < 0.01$) different from that of koenimbine. This result indicates the potent cytotoxic effect of koenimbine in CT-26 cells.

On the other hand, koenimbine did not alter MLC cells' viability significantly up to 25 μg/mL, and at the concentration of 100 μg/mL, the viability of MLC cells was significantly ($^{***}p < 0.001$) reduced to 52% as compared to the control group. Meanwhile, in the koenimbine-treated group, the viability of MLC cells was found to be 69% at the concentration of 50 μg/mL, which is significantly ($^{\#\#}p < 0.01$) different as compared to the 5-FU-treated group (Figure 13). From the above results, koenimbine was found to be nontoxic for MLC cells up to 50 μg/mL with more than 50% cell viability.

These results suggested that koenimbine exhibited significant cytotoxicity against CT-26, but at the same time, koenimbine was found to be nontoxic for MLC cells. In conclusion, koenimbine could be used as a potent anticancer agent for colorectal cancer therapy.

https://doi.org/10.1021/acsomega.2c04051
ACS Omega 2022, 7, 33408−33422

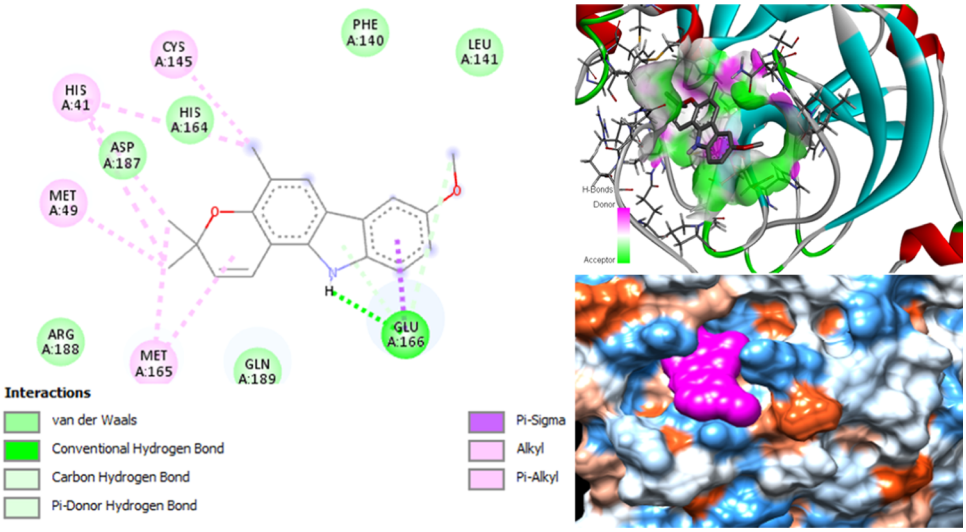

Figure 9. Docking poses of koenimbine with 6LU7.

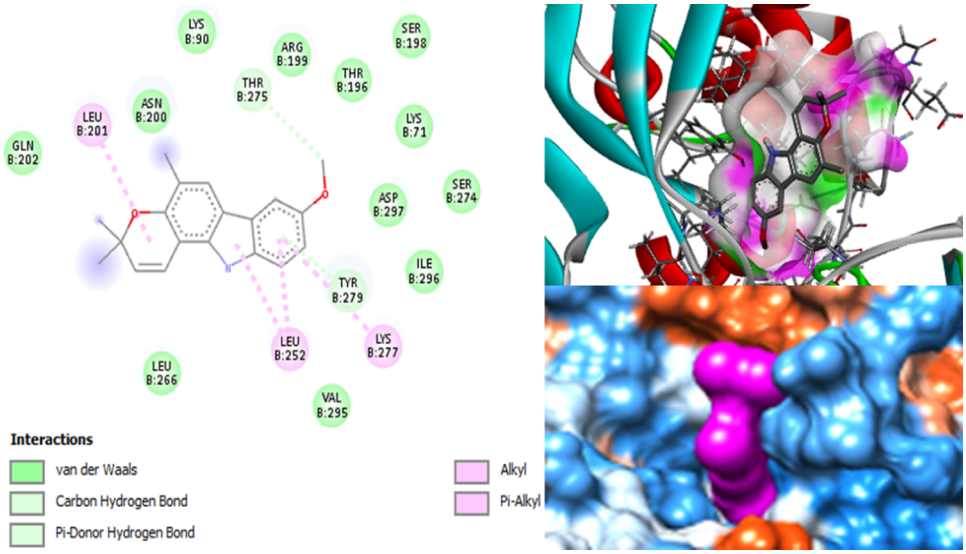

Figure 10. Docking poses of koenimbine with 6VWW.

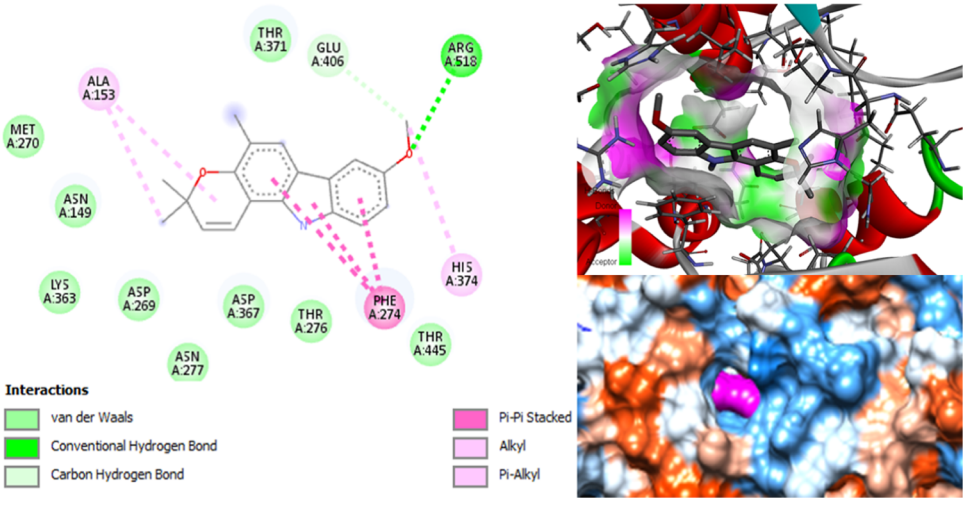

Figure 11. Docking poses of koenimbine with 1R4L.

https://doi.org/10.1021/acsomega.2c04051
ACS Omega 2022, 7, 33408−33422